Chaos, Solitons and Fractals 121 (2019) 108–118

Contents lists available at ScienceDirect

Chaos, Solitons and Fractals

Nonlinear Science, and Nonequilibrium and Complex Phenomena

journal homepage: www.elsevier.com/locate/chaos

Graph-theoretic approach to synchronization of fractional-order coupled systems with time-varying delays via periodically intermittent control

Yao Xu, Yanzhen Li, Wenxue Li*

Department of Mathematics, Harbin Institute of Technology (Weihai), Weihai, 264209, PR China

ARTICLE INFO

Article history:
Received 5 September 2018
Revised 25 January 2019
Accepted 31 January 2019

Keywords:
Synchronization
Fractional-order coupled systems
Time-varying delays
Periodically intermittent control
Graph-theoretic approach

ABSTRACT

This paper deals with synchronization problem of fractional-order coupled systems (FOCSs) with time-varying delays via periodically intermittent control. Here, nonlinear coupling, time-varying internal delay and time-varying coupling delay are considered when modeling, which makes our model more general in comparison with the most existing fractional-order models. It is the first time that periodically intermittent control is applied to synchronizing FOCSs with time-varying delays. Combining Lyapunov method with graph-theoretic approach, some synchronization criteria are obtained. Moreover, the synchronization criteria we derive depend on the fractional order α, control gain, control rate and control period. Besides, the synchronization issues of fractional-order coupled chaotic systems with time-varying delays and fractional-order coupled Hindmarsh–Rose neuron systems with time-varying delays are also investigated as applications of our theoretical results, and relevant sufficient conditions are derived. Finally, numerical simulations with two examples are provided in order to demonstrate the effectiveness of the theoretical results and the feasibility of control strategy.

1. Introduction

In the last decades, coupled systems have received increasing interest due to their impressive applications in various areas. Many of these applications heavily depend on the dynamical behaviors of coupled systems, such as stability [1] and synchronization [2,3]. It is well known that Lyapunov method plays an important role in investigating the dynamical behaviors of coupled systems, and lots of excellent results have been obtained by taking advantage of this method, see [4–6] for example. Nevertheless, in fact, constructing a suitable Lyapunov function is quite difficult. Fortunately, in [7], Li and Shuai proposed a new method (combination of Lyapunov method and graph-theoretic approach) to construct a global Lyapunov function, i.e., the weighted sum of Lyapunov function of each subsystem, which can also make the topological structure of networks be well reflected. Inspired by their work, some scholars have made full use of this method to investigate the dynamical behaviors of coupled systems, and a number of results have been reported [8–10].

It is not difficult to find that most investigations for dynamical behaviors of coupled systems are based on the integer-order dynamical models in aforementioned references. However, in comparison with classical integer-order derivative, a more effective instrument for the description of various materials and processes is provided by fractional-order derivative. And the incorporation of the fractional-order derivative into dynamical systems is an extreme improvement since fractional-order systems possess the characters of non-locality, memory and history-dependent. For instance, the memory of fractional-order systems leads to modeling a fractional-order HIV-immune system in [11]. As many scholars have focused on the dynamical behaviors of fractional-order coupled systems (FOCSs), the synchronization problem of FOCSs has gradually become a hot research point, and a variety of interesting results have been derived, see [12–14] and references therein.

It is noted that time delays sometimes are not taken into consideration in FOCSs, see [15–17] for example. This may be attributed to the fact that it is difficult to extend Lyapunov–Krasovskii functional method, which is frequently used in integer-order coupled systems, to FOCSs directly. However, while working with real phenomena, whether coupling time delay or internal time delay cannot be neglected since they may facilitate the production of undesirable dynamical behaviors such as instability and oscillations [18]. For some FOCSs, generally, constant fixed time delays can serve as good approximation to a certain extent, see [12,19]. Even so, we still cannot ignore the truth that time delays are variable in most situations. Thus, time-varying delays were

* Corresponding author.
E-mail address: wenxuetg@hitwh.edu.cn (W. Li).

https://doi.org/10.1016/j.chaos.2019.01.038
0960-0779/

considered while investigating the synchronization of FOCSs, such as [13,14], which makes their models more realistic. Furthermore, due to the simplicity in its design, coupling forms in most of FOCSs investigated are linear [20,21]. Nevertheless, nonlinear relationship between nodes of coupled systems exists extensively in reality. For example, the coupling form of Kuramoto oscillators model is $\sin(x_j - x_i)$, which is clearly nonlinear. Hence, when investigating the synchronization of FOCSs, nonlinear coupling forms need to be taken into account for the purpose of reasonable modeling. In view of above analysis, nonlinear coupling, time-varying internal delay and time-varying coupling delay are simultaneously considered in our models, and the two kinds of time-varying delays are different from each other, which is more general and realistic.

Recently, synchronization of coupled systems has been successfully achieved via diverse control strategies, such as sampled-data control [22], impulsive control [23], intermittent control [24,25], feedback control [26] and so on. Among these control strategies, the effective and robust intermittent control, which can reduce the amount of transmitted information and save the control cost, has been employed by several researchers to synchronize FOCSs [27–29]. In [27], periodically pinning intermittent control strategy was adopted for synchronization of fractional-order complex dynamical networks. In [29], α-exponential stabilization of fractional-order complex-valued delayed neural networks was considered via periodically intermittent control. However, to the best of our knowledge, only several scholars (see [27–29]) focused on the dynamical behaviors of FOCSs without or with constant fixed time delays via periodically intermittent control. Actually, so far, the investigation of periodically intermittent control for FOCSs with time-varying delays still need to be dedicated. And this paper makes an attempt in this direction for the first time.

Motivated by above discussions, the aim of this paper is to investigate synchronization of FOCSs with time-varying delays under periodically intermittent control. Employing Lyapunov method combined with graph-theoretic approach, some synchronization criteria are obtained. Moreover, our main theoretical results can be applied to fractional-order coupled chaotic systems (FOCCSs) with time-varying delays and fractional-order coupled Hindmarsh–Rose neuron systems (FOCHRNSs) with time-varying delays and synchronization criteria are also derived via periodically intermittent control. The main contributions of this paper are presented as follows.

- Combining Lyapunov method with graph-theoretic approach, periodically intermittent control is applied to synchronizing the FOCSs with time-varying delays for the first time. And applications to FOCCSs with time-varying delays and FOCHRNSs with time-varying delays are also given.
- Nonlinear coupling, time-varying internal delay and time-varying coupling delay are considered into our model, which is more general no matter in theoretical analysis and real applications.
- The synchronization criteria depend on the fractional order, control gain, control rate and control period.

The rest of this paper is organized as follows. In Section 2, preliminaries and model formulation are given. In Section 3, some synchronization criteria are obtained. Applications of our theoretical results are presented in Section 4. In Section 5, numerical simulations are provided. Finally, a conclusion is given in Section 6.

2. Preliminaries and model formulation

For the sake of convenience, some notations will be introduced as follows. Let $\mathbb{M} = \{1, 2, \ldots, m\}$, $\mathbb{N} = \{0, 1, \ldots\}$ and $\mathbb{R}$ represent the set of real numbers. The set of nonnegative real numbers is indicated by $\mathbb{R}^+$. The n-dimensional Euclidean space is denoted as $\mathbb{R}^n$ and $\mathbb{R}^{n\times n}$ signifies the set of $n \times n$ real matrices. Denote the set of complex numbers as $\mathbb{C}$. The superscript "T" denotes the transpose of a matrix or a vector. And $|x| = \sqrt{\sum_{i=1}^{n} x_i^2}$ stands for the Euclidean norm of the vector $x = (x_1, x_2, \ldots, x_n)^{\mathrm{T}} \in \mathbb{R}^n$. Besides, the family of all nonnegative continuous functions $V(t, x)$ which are once differentiable in t and α-order differentiable in x is denoted as $C^{1,\alpha}(\mathbb{R}^+ \times \mathbb{R}^n, \mathbb{R}^+)$. And $C([-\tau, 0], \mathbb{R}^n)$ means the space of continuous functions mapping from $[-\tau, 0]$ into $\mathbb{R}^n$. In addition, some basic knowledge of graph theory can be found in Appendix.

Before formulating the model, a definition for fractional-order derivative will be introduced.

Definition 1 ([30]). The Caputo fractional derivative of order $\alpha \in (n-1, n)$ for an n-order continuous differentiable function $\breve{f}$: $\mathbb{R}^+ \to \mathbb{R}$ is given by

$$ {}_{0}^{C}\mathrm{D}_t^{\alpha} \breve{f}(t) = \frac{1}{\Gamma(n-\alpha)} \int_0^t \frac{\breve{f}^{(n)}(s)}{(t-s)^{\alpha+1-n}} \mathrm{d}s, $$

where $\Gamma(\cdot)$ is the Gamma function given by $\Gamma(q) = \int_0^{\infty} t^{q-1} e^{-t} \mathrm{d}t$. Specially, the Caputo fractional derivative of order $\alpha \in (0, 1)$ for a continuous differentiable function $\breve{f}$: $\mathbb{R}^+ \to \mathbb{R}$ is given by

$$ {}_{0}^{C}\mathrm{D}_t^{\alpha} \breve{f}(t) = \frac{1}{\Gamma(1-\alpha)} \int_0^t \frac{\breve{f}'(s)}{(t-s)^{\alpha}} \mathrm{d}s. $$

For convenience, the Caputo fractional derivative operator ${}_{0}^{C}\mathrm{D}_t^{\alpha}$ is marked as D^{α} in the following discussions.

In what follows, consider FOCSs with time-varying delays modeled on a digraph $\mathcal{G}$ consisting of m nodes, which can be described by

$$ \begin{aligned} \mathrm{D}^{\alpha} x_i(t) = {} & f(x_i(t), x_i(t-\tau_1(t))) + \sum_{j=1}^{m} a_{ij} H_{ij}(x_j(t-\tau_2(t)) \\ & - x_i(t-\tau_2(t))) + u_i(t), \quad i \in \mathbb{M}, \end{aligned} \tag{1} $$

where $0 < \alpha < 1$, and $x_i(t) = (x_{i1}(t), x_{i2}(t), \ldots, x_{in}(t))^{\mathrm{T}} \in \mathbb{R}^n$ is state vector of the ith node. Vector-valued function $f : \mathbb{R}^n \times \mathbb{R}^n \to \mathbb{R}^n$ is continuous. And $\tau_1(t)$, $\tau_2(t)$ stand for time-varying delays, which may be unknown but are bounded by a positive constant, that is $0 \le \tau_1(t), \ \tau_2(t) \le \tau$, where $\tau_1(t)$ denotes the time-varying internal delay, and $\tau_2(t)$ denotes the time-varying coupling delay. In addition, $H_{ij} : \mathbb{R}^n \to \mathbb{R}^n$ is a coupling form which means the influence of the jth node on the ith node, and the nonnegative constant a_{ij} represents coupling strength. If there exists an arc (j, i) in $\mathcal{G}$, then $a_{ij} > 0$, otherwise $a_{ij} = 0$. Besides, $u_i(t)$ is control input, which will be illustrated in detail in Section 3.

Define the solution of system (1) as $x(t) = \left(x_1^{\mathrm{T}}(t), x_2^{\mathrm{T}}(t), \ldots, x_m^{\mathrm{T}}(t)\right)^{\mathrm{T}} \in \mathbb{R}^{nm}$, and the initial conditions associated with system (1) are given by $\chi(t) = \left(\chi_1^{\mathrm{T}}(t), \chi_2^{\mathrm{T}}(t), \ldots, \chi_m^{\mathrm{T}}(t)\right)^{\mathrm{T}} \in C([-\tau, 0], \mathbb{R}^{nm})$. Assume that $x(t) \equiv 0$ is an equilibrium point, otherwise, through a change of variables, the equilibrium point can be shifted to the origin.

Remark 1. It is noted that in some literature, such as [20,21], the coupling forms were considered to be linear. Besides, in [13,31], nonlinear coupling form $f_j(x_j)$ which is independent of x_i was considered. However, in reality, the coupling form is usually supposed to be nonlinear, and it ought to be associated with both x_j and x_i as well. For instance, in the model of the Kuramoto oscillators network established in [8], the coupling form is $\sin(x_j - x_i)$. Compared with aforementioned references, in this paper, the nonlinear coupling form $H_{ij}(x_j - x_i)$ related to both x_j and x_i is considered, which is more practical.

Suppose $s(t) = (s_1(t), s_2(t), \ldots, s_n(t))^{\mathrm{T}} \in \mathbb{R}^n$ is a solution of an isolated node satisfying

$$ \mathrm{D}^{\alpha} s(t) = f(s(t), s(t-\tau_1(t))), \tag{2} $$

where synchronization state $s(t)$ can be an equilibrium point, a nontrivial periodic orbit, or even a chaotic orbit. The initial conditions associated with system (2) are given by $\gamma(t) = (\gamma_1(t), \gamma_2(t), \ldots, \gamma_n(t))^{\mathrm{T}} \in C([-\tau, 0], \mathbb{R}^n)$.

Define error vector as $e_i(t) = x_i(t) - s(t), i \in \mathbb{M}$, then synchronization error system can be described as

$$\begin{aligned} \mathrm{D}^\alpha e_i(t) &= f(x_i(t), x_i(t-\tau_1(t))) - f(s(t), s(t-\tau_1(t))) \\ &\quad + \sum_{j=1}^{m} a_{ij} H_{ij}(x_j(t-\tau_2(t)) - x_i(t-\tau_2(t))) + u_i(t), i \in \mathbb{M}. \end{aligned} \tag{3}$$

Next, a definition of global synchronization will be given.

Definition 2. System (1) can achieve global synchronization if for initial conditions $\chi(t) \in C([-\tau, 0], \mathbb{R}^{nm})$ and $\gamma(t) \in C([-\tau, 0], \mathbb{R}^n)$, the following equation holds:

$$\lim_{t\to\infty} |e(t)| = 0,$$

where $e(t) = \left(e_1^{\mathrm{T}}(t), e_2^{\mathrm{T}}(t), \ldots, e_m^{\mathrm{T}}(t)\right)^{\mathrm{T}} \in \mathbb{R}^{nm}$.

Subsequently, in order to obtain main results of this paper, an assumption, a property, a definition with a lemma are provided successively as follows.

Assumption 1. For any $i, j \in \mathbb{M}$, $x \in \mathbb{R}^n$, there exists a positive constant δ_{ij} such that

$$|H_{ij}(x)| \le \delta_{ij}|x|.$$

Property 1 *([30]). For any constants $\bar{\upsilon}_1$ and $\bar{\upsilon}_2$, the linearity of Caputo fractional derivative is described by*

$$\mathrm{D}^\alpha(\bar{\upsilon}_1 f(t) + \bar{\upsilon}_2 g(t)) = \bar{\upsilon}_1 \mathrm{D}^\alpha f(t) + \bar{\upsilon}_2 \mathrm{D}^\alpha g(t).$$

Definition 3 ([30]). For $\alpha, \beta \in \mathbb{C}$, the Mittag–Leffler function in two parameters is defined as

$$E_{\alpha,\beta}[z] = \sum_{k=0}^{\infty} \frac{z^k}{\Gamma(k\alpha + \beta)}.$$

$$\mathrm{D}^\alpha V_i(t, e_i(t)) \le \begin{cases} -\lambda_i V_i(t, e_i(t)) + \displaystyle\sum_{k=1}^{2} \xi_i V_i(t-\tau_k(t), e_i(t-\tau_k(t))) \\ + \displaystyle\sum_{j=1}^{m} \hat{a}_{ij} F_{ij}(e_i(t-\tau_2(t)), e_j(t-\tau_2(t))), & lT \le t \le (l+\varpi)T, \\ \bar{\lambda}_i V_i(t, e_i(t)) + \displaystyle\sum_{k=1}^{2} \xi_i V_i(t-\tau_k(t), e_i(t-\tau_k(t))) \\ + \displaystyle\sum_{j=1}^{m} \hat{a}_{ij} F_{ij}(e_i(t-\tau_2(t)), e_j(t-\tau_2(t))), & (l+\varpi)T < t < (l+1)T, \end{cases} \quad l \in \mathbb{N}.$$

When $\beta = 1$ and $\alpha > 0$, the Mittag–Leffler function can be written in a special case as

$$E_\alpha[z] = \sum_{k=0}^{\infty} \frac{z^k}{\Gamma(k\alpha + 1)}.$$

Lemma 1 *([30]). Suppose that $x(t) \in \mathbb{R}^n$ is a continuous and differentiable vector-valued function, $\mathbf{P} \in \mathbb{R}^{n\times n}$ is a positive definite real matrix. Then for quadratic function $x^{\mathrm{T}}(t)\mathbf{P}x(t)$, we have*

$$\mathrm{D}^\alpha x^{\mathrm{T}}(t)\mathbf{P}x(t) \le 2x^{\mathrm{T}}(t)\mathbf{P}\mathrm{D}^\alpha x(t), \quad \alpha \in (0, 1).$$

3. Main results

The synchronization problem of system (1) will be considered in this section. In order to realize synchronization of system (1), consider the following periodically intermittent control which can be depicted as

$$u_i(t) = \begin{cases} -d_i e_i(t), & lT \le t \le (l+\varpi)T, \\ 0, & (l+\varpi)T < t < (l+1)T, \end{cases} \quad l \in \mathbb{N}, i \in \mathbb{M}, \tag{4}$$

in which control gain d_i is a positive constant, $T > 0$ is the control period, $\varpi \in (0, 1)$ is called control rate, ϖT is the so-called control width.

Remark 2. At present, some continuous control schemes are put forward to realize the synchronization of coupled systems, such as feedback control [32], pinning control [19], adaptive control [21] and so on. However, in some practical fields, considering cost and economic benefits, many implementers show their preference to discontinuous control (including intermittent control, impulsive control, etc.). To some extent, the continuous control method is not reasonable, and extra cost may be produced, such as microgrid control and wind energy conversion control [6]. Compared with impulsive control [33,34], intermittent control has nonzero control width, which means intermittent control is easier to be implemented in practical engineering problems. It should be noticed that periodically intermittent control has been widely employed to synchronize integer-order systems, and a great deal of interesting results have been obtained. Nevertheless, few papers discuss the fractional-order case with time-varying delays. Hence, this paper makes an attempt in this direction for the first time.

In what follows, some sufficient conditions will be presented.

Theorem 1. *System (1) can achieve global synchronization if the following conditions are satisfied.*

A1 There exists a function $V_i(t, e_i) \in C^{1,\alpha}(\mathbb{R}^+ \times \mathbb{R}^n, \mathbb{R}^+)$ $(i \in \mathbb{M})$ satisfying:

(i) *There exists a positive constant υ_i such that $\upsilon_i|e_i|^2 \le V_i(t, e_i)$.*

(ii) *There exist positive constants λ_i, $\bar{\lambda}_i$, ξ_i, a nonnegative constant $\hat{a}_{ij}$ and a function F_{ij} such that*

A2 Along each directed cycle $\mathcal{C}_Q$ of strongly connected digraph $(\mathcal{G}, \hat{A})$, where $\hat{A} = (\hat{a}_{ij})_{m\times m}$, it satisfies

$$\sum_{(s,r)\in\mathbb{E}(\mathcal{C}_Q)} F_{rs}(e_r, e_s) \le 0. \tag{5}$$

A3 There exist positive constants θ_1 and θ_2 such that

$$E_\alpha[-\theta_1 \varpi^\alpha T^\alpha] E_\alpha[\theta_2(1-\varpi)^\alpha T^\alpha] < 1,$$

where $\lambda - 2\xi \ge \theta_1$, $\bar{\lambda} + 2\xi \le \theta_2$, $\lambda = \min_{i\in\mathbb{M}}\{\lambda_i\}$, $\xi = \max_{i\in\mathbb{M}}\{\xi_i\}$, and $\bar{\lambda} = \max_{i\in\mathbb{M}}\{\bar{\lambda}_i\}$.

Proof. Construct a Lyapunov function as follows:

$$V(t, e) = \sum_{i=1}^{m} c_i V_i(t, e_i),$$

in which c_i is the cofactor of the ith diagonal element of the Laplacian matrix of digraph $(\mathcal{G}, \hat{A})$. Since digraph $(\mathcal{G}, \hat{A})$ is strongly connected, according to Lemma 2 (see Appendix), we get $c_i > 0$. Furthermore, on the basis of condition A1(i), it yields that

$$V(t,e) = \sum_{i=1}^{m} c_i V_i(t,e_i) \geq \sum_{i=1}^{m} c_i \upsilon_i |e_i|^2 \geq \min_{i\in\mathbb{M}}\{c_i\upsilon_i\} \sum_{i=1}^{m} |e_i|^2 = \upsilon |e|^2, \tag{6}$$

where $\upsilon = \min_{i\in\mathbb{M}}\{c_i\upsilon_i\}$. On the one hand, when $lT \leq t \leq (l+\varpi)T$, in terms of condition A1(ii) and Property 1, we can derive

$$\begin{aligned} \mathrm{D}^{\alpha}V(t,e(t)) &= \sum_{i=1}^{m} c_i \mathrm{D}^{\alpha} V_i(t,e_i(t)) \\ &\leq -\sum_{i=1}^{m} c_i\lambda_i V_i(t,e_i(t)) \\ &\quad + \sum_{i=1}^{m}\sum_{k=1}^{2} c_i\xi_i V_i(t-\tau_k(t), e_i(t-\tau_k(t))) \\ &\quad + \sum_{i=1}^{m}\sum_{j=1}^{m} c_i\hat{a}_{ij}F_{ij}(e_i(t-\tau_2(t)), e_j(t-\tau_2(t))) \end{aligned}$$

According to Lemma 2 and condition A2, it can be obtained that

$$\sum_{i=1}^{m}\sum_{j=1}^{m} c_i\hat{a}_{ij}F_{ij}(e_i,e_j) = \sum_{\mathcal{Q}\in\mathbb{Q}} W(\mathcal{Q}) \sum_{(s,r)\in\mathbb{E}(\mathcal{C}_{\mathcal{Q}})} F_{rs}(e_r,e_s) \leq 0. \tag{7}$$

It follows that

$$\begin{aligned} \mathrm{D}^{\alpha}V(t,e(t)) &\leq -\min_{i\in\mathbb{M}}\{\lambda_i\} V(t,e(t)) \\ &\quad + \max_{i\in\mathbb{M}}\{\xi_i\} \sum_{k=1}^{2} V(t-\tau_k(t), e(t-\tau_k(t))) \\ &\leq -\lambda V(t,e(t)) + 2\xi \sup_{t-\tau\leq s\leq t} V(s,e(s)). \end{aligned} \tag{8}$$

Estimated by (8), for the solution $e(t)$ of system (3), which satisfies the Razumikhin condition

$$V(s,e(s)) \leq V(t,e(t)), \quad t-\tau \leq s \leq t,$$

we have

$$\mathrm{D}^{\alpha}V(t,e(t)) \leq -(\lambda - 2\xi)V(t,e(t)).$$

By virtue of condition A3, we arrive at

$$\mathrm{D}^{\alpha}V(t,e(t)) \leq -\theta_1 V(t,e(t)).$$

On the other hand, when $(l+\varpi)T < t < (l+1)T$, analogously, combined with (7), it follows that

$$\begin{aligned} \mathrm{D}^{\alpha}V(t,e(t)) &= \sum_{i=1}^{m} c_i \mathrm{D}^{\alpha} V_i(t,e_i(t)) \leq \sum_{i=1}^{m} c_i\bar{\lambda}_i V_i(t,e_i(t)) \\ &\quad + \sum_{i=1}^{m}\sum_{k=1}^{2} c_i\xi_i V_i(t-\tau_k(t), e_i(t-\tau_k(t))) \\ &\quad + \sum_{i=1}^{m}\sum_{j=1}^{m} c_i\hat{a}_{ij}F_{ij}(e_i(t-\tau_2(t)), e_j(t-\tau_2(t))) \\ &\leq \max_{i\in\mathbb{M}}\{\lambda_i\} V(t,e(t)) \\ &\quad + \max_{i\in\mathbb{M}}\{\xi_i\} \sum_{k=1}^{2} V(t-\tau_k(t), e(t-\tau_k(t))) \\ &\leq \bar{\lambda} V(t,e(t)) + 2\xi \sup_{t-\tau\leq s\leq t} V(s,e(s)). \end{aligned}$$

From the above estimation, if the solution $e(t)$ of system (3) satisfies the Razumikhin condition

$$V(s,e(s)) \leq V(t,e(t)), \ t-\tau \leq s \leq t,$$

we can derive

$$\mathrm{D}^{\alpha}V(t,e(t)) \leq (\bar{\lambda} + 2\xi)V(t,e(t)).$$

By condition A3, it yields

$$\mathrm{D}^{\alpha}V(t,e(t)) \leq \theta_2 V(t,e(t)).$$

In conclusion, it can be checked that

$$\mathrm{D}^{\alpha}V(t,e(t)) \leq \begin{cases} -\theta_1 V(t,e(t)), & lT \leq t \leq (l+\varpi)T, \\ \theta_2 V(t,e(t)), & (l+\varpi)T < t < (l+1)T, \end{cases} \ l \in \mathbb{N}.$$

In the following, the detailed process of proof will be clarified by using induction. When $t \in [0, \varpi T]$, it follows from $\mathrm{D}^{\alpha}V(t,e(t)) \leq -\theta_1 V(t,e(t))$, there is a nonnegative function $\Xi(t)$, such that

$$\mathrm{D}^{\alpha}V(t,e(t)) + \theta_1 V(t,e(t)) + \Xi(t) = 0. \tag{9}$$

Taking the Laplace transform on both sides of (9), it yields that

$$s^{\alpha}\mathcal{L}[V(t,e(t))] - s^{\alpha-1}\mathcal{L}[V(0,e(0))] + \theta_1\mathcal{L}[V(t,e(t))] + \mathcal{L}[\Xi(t)] = 0,$$

where $\mathcal{L}[\cdot]$ denotes the Laplace transform of a function. Then we can obtain that

$$\mathcal{L}[V(t,e(t))] = \frac{s^{\alpha-1}\mathcal{L}[V(0,e(0))] - \mathcal{L}[\Xi(t)]}{s^{\alpha}+\theta_1}. \tag{10}$$

Taking inverse Laplace transform on both sides of (10), we get

$$V(t,e(t)) = V(0,e(0))E_{\alpha}[-\theta_1 t^{\alpha}] - \Xi(t) * \{t^{\alpha-1}E_{\alpha,\alpha}[-\theta_1 t^{\alpha}]\},$$

in which $*$ represents the convolution operator. Notice that $t^{\alpha-1}$ and $E_{\alpha,\alpha}[-\theta_1 t^{\alpha}]$ are nonnegative functions, it is clear that

$$V(t,e(t)) \leq V(0,e(0))E_{\alpha}[-\theta_1 t^{\alpha}],$$

and $V(\varpi T, e(\varpi T)) = V(0,e(0))E_{\alpha}[-\theta_1(\varpi T)^{\alpha}]$.

And by using the similar iterative method, when $t \in (\varpi T, T)$, one can obtain that

$$\begin{aligned} V(t,e(t)) &\leq V(\varpi T, e(\varpi T))E_{\alpha}[\theta_2(t-\varpi T)^{\alpha}] \\ &\leq V(0,e(0))E_{\alpha}[-\theta_1(\varpi T)^{\alpha}]E_{\alpha}[\theta_2(t-\varpi T)^{\alpha}]. \end{aligned}$$

When $t \in [T, (1+\varpi)T]$, we have

$$\begin{aligned} V(t,e(t)) &\leq V(T,e(T))E_{\alpha}[-\theta_1(t-T)^{\alpha}] \\ &\leq V(0,e(0))E_{\alpha}[-\theta_1\varpi^{\alpha}T^{\alpha}]E_{\alpha}[\theta_2((1-\varpi)T)^{\alpha}] \\ &\quad E_{\alpha}[-\theta_1(t-T)^{\alpha}]. \end{aligned}$$

When $t \in ((1+\varpi)T, 2T)$, one can get

$$\begin{aligned} V(t,e(t)) &\leq V((1+\varpi)T, e((1+\varpi)T))E_{\alpha}[\theta_2(t-(1+\varpi)T)^{\alpha}] \\ &\leq V(0,e(0))E_{\alpha}[-\theta_1\varpi^{\alpha}T^{\alpha}]E_{\alpha}[\theta_2((1-\varpi)T)^{\alpha}] \\ &\quad E_{\alpha}[-\theta_1\varpi^{\alpha}T^{\alpha}]E_{\alpha}[\theta_2(t-(1+\varpi)T)^{\alpha}]. \end{aligned}$$

Using induction, when $t \in [lT, (l+\varpi)T]$, it yields

$$\begin{aligned} V(t,e(t)) &\leq V(lT, e(lT))E_{\alpha}[-\theta_1(t-lT)^{\alpha}] \\ &\leq V(0,e(0))(E_{\alpha}[-\theta_1\varpi^{\alpha}T^{\alpha}]E_{\alpha}[\theta_2(1-\varpi)^{\alpha}T^{\alpha}])^{l} \\ &\quad E_{\alpha}[-\theta_1(t-lT)^{\alpha}]. \end{aligned}$$

It is notable that when $t \in [lT, (l+\varpi)T]$, $x \leq 0$ and $0 < \alpha < 1$, according to [27], we have $0 < E_{\alpha}[x] \leq 1$. Hence, we can derive that

$$V(t,e(t)) \leq V(0,e(0))(E_{\alpha}[-\theta_1\varpi^{\alpha}T^{\alpha}]E_{\alpha}[\theta_2(1-\varpi)^{\alpha}T^{\alpha}])^{l}. \tag{11}$$

When $t \in ((l+\varpi)T, (l+1)T)$, we arrive at

$$V(t,e(t)) \le V((l+\varpi)T, e((l+\varpi)T))E_\alpha[\theta_2(t-(l+\varpi)T)^\alpha]$$
$$\le V(0,e(0))(E_\alpha[-\theta_1\varpi^\alpha T^\alpha]E_\alpha[\theta_2(1-\varpi)^\alpha T^\alpha])^l$$
$$E_\alpha[\theta_2(t-(l+\varpi)T)^\alpha]E_\alpha[-\theta_1\varpi^\alpha T^\alpha].$$

In the same way, under the circumstance of $t \in ((l+\varpi)T, (l+1)T)$, $x \le 0$ and $0<\alpha<1$, according to [27], there is $0 < E_\alpha[x] \le 1$. And following inequality holds:

$$V(t,e(t)) \le V(0,e(0))(E_\alpha[-\theta_1\varpi^\alpha T^\alpha]E_\alpha[\theta_2(1-\varpi)^\alpha T^\alpha])^l$$
$$E_\alpha[\theta_2(1-\varpi)^\alpha T^\alpha]. \tag{12}$$

When $t\to\infty$, it implies that $l\to\infty$. Meanwhile, according to condition A3, inequalities (11) and (12), we can show that $\lim_{t\to\infty} V(t,e(t)) = 0$. Because of (6), it is easy to obtain that $\lim_{t\to\infty}|e(t)| = 0$. Hence, in view of Definition 2, system (1) can reach global synchronization. This completes the proof. □

Remark 3. At present, some scholars have derived some synchronization criteria of FOCSs by estimating the solutions directly [35,36]. In fact, Lyapunov method is an effective approach to investigating dynamical behaviors, and lots of interesting results were obtained by using this method [4–6]. However, the Lyapunov function they constructed cannot well reflect the topological structure of networks. With a view to constructing a global Lyapunov function based on the Lyapunov function of each subsystem and topological structure of networks, we adopt the technique of combining Lyapunov method with graph-theoretic approach, which was proposed by Li et al. in [7], and sufficient conditions for synchronization of FOCSs are obtained successfully.

Remark 4. In this paper, different from those papers neglecting time delays [15–17] or considering constant fixed time delays [12,19], time-varying delays including time-varying internal delay and time-varying coupling delay are considered due to their effects on synchronization in practice. The incorporation of fractional calculus is beneficial to reasonably modeling the practical systems, but it brings additional obstacles for dynamical analysis of systems. As is known to all, Lyapunov–Krasovskii functional method is frequently used to investigate dynamical behaviors of integer-order delayed coupled systems. But there still exist some difficulties in extending this method to FOCSs directly at present. Some scholars used comparison principle to obtain synchronization criteria of FOCSs with time delays [19,37]. Different from their method, in this paper, we present the Razumikhin condition to overcome aforementioned difficulties, which is known as Razumikhin technique [13,32].

Remark 5. Denote $g(\varpi) = E_\alpha[-\theta_1\varpi^\alpha T^\alpha]E_\alpha[\theta_2(1-\varpi)^\alpha T^\alpha] - 1$, where $\varpi \in (0, 1)$. It follows that $E_\alpha[-\theta_1\varpi^\alpha T^\alpha]$ and $E_\alpha[\theta_2(1-\varpi)^\alpha T^\alpha]$ are nonnegative and strictly decreasing continuous functions of ϖ. Therefore, $g(\varpi)$ is a strictly decreasing continuous function of ϖ. Since $g(0) = E_\alpha[\theta_2 T^\alpha] - 1 > 0$ and $g(1) = E_\alpha[-\theta_1 T^\alpha] < 0$, we know that there exists a unique $\varpi \in (0, 1)$ such that $g(\varpi) = 0$. Combined with the continuity of $g(\varpi)$, inequality $E_\alpha[-\theta_1\varpi^\alpha T^\alpha]E_\alpha[\theta_2(1-\varpi)^\alpha T^\alpha] < 1$ in Theorem 1 can be hold.

Remark 6. Sometimes, it is not easy to verify condition A2 in Theorem 1 on account of the existence of numerous directed cycles. Fortunately, according to [7], if there exists a function $G(\cdot)$ such that

$$F_{ij}(e_i, e_j) \le G(e_j) - G(e_i), \quad i, j \in \mathbb{M}, \tag{13}$$

then inequality (5) can be easily verified.

Based on an argument about a Lyapunov function, Theorem 1 has been obtained. Nevertheless, it is troublesome to construct an appropriate Lyapunov function. Thus, placing certain conditions on the coefficients of system (1) is of great help for theoretical analysis. Next, some sufficient conditions will be presented as an attempt in this direction.

Theorem 2. *Suppose that Assumption 1 holds, and digraph $(\mathcal{G}, A)$, where $A = (a_{ij})_{m\times m}$, is strongly connected. System (1) can achieve global synchronization if the following conditions are satisfied.*

B1 *There exist nonnegative constants Λ and μ such that*

$$(x_i - s)^{\mathrm{T}}[f(x_i,\tilde{x}_i) - f(s,\tilde{s})] \le \Lambda|x_i - s|^2 + \mu|\tilde{x}_i - \tilde{s}|^2.$$

B2 *There exist positive constants θ_1 and θ_2 such that*

$$E_\alpha[-\theta_1\varpi^\alpha T^\alpha]E_\alpha[\theta_2(1-\varpi)^\alpha T^\alpha] < 1,$$

where $\lambda - 2\xi \ge \theta_1$, $\bar{\lambda} + 2\xi \le \theta_2$, $\lambda = \min_{i\in\mathbb{M}}\{\lambda_i\}$, $\xi = \max_{i\in\mathbb{M}}\{\xi_i\}$, $\bar{\lambda} = \max_{i\in\mathbb{M}}\{\bar{\lambda}_i\}$, $\bar{\lambda}_i = 2\left(\Lambda + \sum_{j=1}^m a_{ij}\delta_{ij}\right)$, $\lambda_i = 2\left(d_i - \Lambda - \sum_{j=1}^m a_{ij}\delta_{ij}\right) > 0$, *and* $\xi_i = \max\left\{2\mu, 2\sum_{j=1}^m a_{ij}\delta_{ij}\right\}$.

Proof. Define a function as

$$V_i(t, e_i) = e_i^{\mathrm{T}} e_i.$$

It is obvious that condition A1(i) in Theorem 1 is satisfied. When $lT \le t \le (l+\varpi)T$, by virtue of Lemma 1, it yields that

$$\begin{aligned}
\mathrm{D}^\alpha V_i(t, e_i(t)) &\le 2e_i^{\mathrm{T}}(t)\Bigg[f(x_i(t), x_i(t-\tau_1(t))) - f(s(t), s(t-\tau_1(t)))\\
&\quad + \sum_{j=1}^m a_{ij}H_{ij}(x_j(t-\tau_2(t)) - x_i(t-\tau_2(t))) + u_i(t)\Bigg]\\
&\le 2\Lambda|e_i(t)|^2 + 2\mu|e_i(t-\tau_1(t))|^2 - 2d_i|e_i(t)|^2\\
&\quad + 2|e_i(t)|\sum_{j=1}^m a_{ij}|H_{ij}(e_j(t-\tau_2(t)) - e_i(t-\tau_2(t)))|\\
&\le 2(\Lambda - d_i)|e_i(t)|^2 + 2\mu|e_i(t-\tau_1(t))|^2\\
&\quad + 2\sum_{j=1}^m a_{ij}\delta_{ij}|e_i(t)||e_j(t-\tau_2(t)) - e_i(t-\tau_2(t))|\\
&\le 2\left(\Lambda - d_i + \sum_{j=1}^m a_{ij}\delta_{ij}\right)|e_i(t)|^2 + 2\mu|e_i(t-\tau_1(t))|^2\\
&\quad + 2\sum_{j=1}^m a_{ij}\delta_{ij}|e_i(t-\tau_2(t))|^2\\
&\quad + \sum_{j=1}^m a_{ij}\delta_{ij}\left(|e_j(t-\tau(t))|^2 - |e_i(t-\tau_2(t))|^2\right)\\
&\le -\lambda_i|e_i(t)|^2 + \sum_{k=1}^2 \xi_i|e_i(t-\tau_k(t))|^2\\
&\quad + \sum_{j=1}^m a_{ij}\delta_{ij}\left(|e_j(t-\tau_2(t))|^2 - |e_i(t-\tau_2(t))|^2\right)\\
&= -\lambda_i V_i(t, e_i(t)) + \sum_{k=1}^2 \xi_i V_i(t-\tau_k(t), e_i(t-\tau_k(t)))\\
&\quad + \sum_{j=1}^m \hat{a}_{ij}F_{ij}(e_i(t-\tau_2(t)), e_j(t-\tau_2(t))),
\end{aligned} \tag{14}$$

where $\hat{a}_{ij} = a_{ij}\delta_{ij}$, $F_{ij}(e_i, e_j) = |e_j|^2 - |e_i|^2$, which satisfies (13). Besides, analogously, it is easy to get that when $(l+\varpi)T < t < (l+$

1)T, we have

$$\begin{aligned}\mathrm{D}^{\alpha}V_i(t,e_i(t)) \leq\, & 2e_i^{\mathrm{T}}(t)\Bigg[f(x_i(t),x_i(t-\tau_1(t)))-f(s(t),s(t-\tau_1(t)))\\ & +\sum_{j=1}^{m}a_{ij}H_{ij}(x_j(t-\tau_2(t))-x_i(t-\tau_2(t)))\Bigg]\\ \leq\, & 2\left(\Lambda+\sum_{j=1}^{m}a_{ij}\delta_{ij}\right)|e_i(t)|^2+2\mu|e_i(t-\tau_1(t))|^2\\ & +2\sum_{j=1}^{m}a_{ij}\delta_{ij}|e_i(t-\tau_2(t))|^2\\ & +\sum_{j=1}^{m}a_{ij}\delta_{ij}\left(|e_j(t-\tau_2(t))|^2-|e_i(t-\tau_2(t))|^2\right)\\ \leq\, & \bar{\lambda}_iV_i(t,e_i(t))+\sum_{k=1}^{2}\xi_iV_i(t-\tau_k(t),e_i(t-\tau_k(t)))\\ & +\sum_{j=1}^{m}\hat{a}_{ij}F_{ij}(e_i(t-\tau_2(t)),e_j(t-\tau_2(t))). \qquad (15)\end{aligned}$$

Combining (14) with (15), we know that condition A1(ii) in Theorem 1 is satisfied. Moreover, due to the fact that digraph $(\mathcal{G},A)$ is strongly connected and $\delta_{ij}>0$, we know digraph $(\mathcal{G},\hat{A})$ is strongly connected, where $\hat{A}=(\hat{a}_{ij})_{m\times m}$, which implies condition A2 in Theorem 1 is satisfied. Combined with conditions in Theorem 2, all conditions in Theorem 1 are satisfied. Hence, we can conclude that system (1) can achieve the global synchronization. This completes the proof. □

Remark 7. As a matter of fact, two theorems proposed in this section are closely related. Theorem 1 is obtained by constructing a global Lyapunov function based on the Lyapunov function of each subsystem and topological structure of networks. In order to show that such Lyapunov function of subsystem exists, Theorem 2 is presented. Furthermore, Theorem 2 presents a synchronization criterion based on coefficients of system (1), which is more convenient to investigate the synchronization of practical systems. Compared with some relevant literature, such as [38,39], in this paper, there is no necessity to solve any linear matrix inequality, and all we need is to verify the conditions based on coefficients of system (1), which is undoubtedly an easier task.

Remark 8. In terms of condition B2 in Theorem 2, it is clear that our synchronization criteria are related to the order α of FOCSs, control gain d_i, control rate ϖ and control period T. In detail, when other parameters are fixed, the larger control gain d_i or the smaller coupling strength a_{ij} is, the easier conditions are satisfied. However, in practice, control gain d_i is unrealistic to be very large which may contribute to the high control cost and the difficulty of real implementations. Hence, in condition B2, the lower bound of control gain d_i is given, i.e., $d_i>\Lambda+\sum_{j=1}^{m}a_{ij}\delta_{ij}$.

4. Applications

4.1. Synchronization of fractional-order coupled chaotic systems with time-varying delays

As time goes by, FOCSs have drawn considerable attention and been widely used in the fields of relaxation, oscillation and control. Thereinto, fractional-order chaotic systems have aroused widespread interest and in-depth researches [40]. The researches and developments of fractional-order chaotic systems have been promoted as the presences of the fractional-order Chua's circuits, Rossler systems, Chen systems, Lorenz systems, Liu systems, Lü systems, etc. The fractional-order chaotic systems have been applied in a variety of applications. For example, in terms of secure communication and signal processing, fractional-order chaotic systems will be more confidential and with higher anti-broken capability than the integer-order chaotic systems. In view of this fact, it is of great significance to promote the researches of fractional-order chaotic systems. Then unified fractional-order chaotic systems are given as follows.

$$\begin{cases}\mathrm{D}^{\alpha}x_{i1}(t)=\alpha_1(x_{i2}(t)-x_{i1}(t)),\\ \mathrm{D}^{\alpha}x_{i2}(t)=\alpha_2x_{i1}(t)-x_{i1}(t)x_{i3}(t)+\alpha_3x_{i2}(t), & i\in\mathbb{M},\\ \mathrm{D}^{\alpha}x_{i3}(t)=x_{i1}(t)x_{i2}(t)-\alpha_4x_{i3}(t),\end{cases}$$

where $0<\alpha<1$, $\alpha_1=25\zeta+10$, $\alpha_2=28-35\zeta$, $\alpha_3=29\zeta-1$, $\alpha_4=(8+\zeta)/3$ and $\zeta\in[0,\ 1]$. Let $x_i(t)=(x_{i1}(t),x_{i2}(t),x_{i3}(t))^{\mathrm{T}}$ be the ith state vector, and set

$$f(x_i(t),x_i(t-\tau_1(t)))=\begin{pmatrix}\alpha_1(x_{i2}(t)-x_{i1}(t))\\ \alpha_2x_{i1}(t)-x_{i1}(t)x_{i3}(t)+\alpha_3x_{i2}(t)\\ x_{i1}(t)x_{i2}(t)-\alpha_4x_{i3}(t)\end{pmatrix}.$$

In what follows, taking nonlinear coupling, time-varying delays and periodically intermittent controller (4) into consideration, FOCCSs with time-varying delays can be described as

$$\begin{aligned}\mathrm{D}^{\alpha}x_i(t)=\, & f(x_i(t),x_i(t-\tau_1(t)))+\sum_{j=1}^{m}a_{ij}H_{ij}(x_j(t-\tau_2(t))\\ & -x_i(t-\tau_2(t)))+u_i(t),\quad i\in\mathbb{M}, \qquad (16)\end{aligned}$$

where $0<\alpha<1$, the nonnegative constant a_{ij} stands for the coupling strength, $H_{ij}:\mathbb{R}^3\to\mathbb{R}^3$ is the coupling form, $\tau_1(t)=0$, $\tau_2(t)$ is the time-varying coupling delay which is bounded by a positive constant τ, that is $0\leq\tau_2(t)\leq\tau$.

Let $s(t)=(s_1(t),s_2(t),s_3(t))^{\mathrm{T}}$, and suppose that $s(t)$ is a solution of an isolated node satisfying

$$\mathrm{D}^{\alpha}s(t)=f(s(t),s(t-\tau_1(t))).$$

The attractor of the isolated node is bounded, i.e., $|s_k(t)|\leq p_k$, $k=1,2,3$.

Define error vector as $e_i(t)=x_i(t)-s(t), i\in\mathbb{M}$, then error system can be derived:

$$\begin{aligned}\mathrm{D}^{\alpha}e_i(t)=\, & f(x_i(t),x_i(t-\tau_1(t)))-f(s(t),s(t-\tau_1(t)))\\ & +\sum_{j=1}^{m}a_{ij}H_{ij}(x_j(t-\tau_2(t))-x_i(t-\tau_2(t)))+u_i(t),\quad i\in\mathbb{M}.\end{aligned}$$

The following sufficient conditions are given to guarantee the global synchronization of system (16).

Theorem 3. *Suppose that Assumption 1 holds, and digraph $(\mathcal{G},A)$, where $A=(a_{ij})_{m\times m}$, is strongly connected. System (16) can achieve global synchronization if there exist positive constants θ_1 and θ_2 such that*

$$E_{\alpha}[-\theta_1\varpi^{\alpha}T^{\alpha}]E_{\alpha}[\theta_2(1-\varpi)^{\alpha}T^{\alpha}]<1,$$

where $\lambda-2\xi\geq\theta_1$, $\bar{\lambda}+2\xi\leq\theta_2$, $\lambda=\min_{i\in\mathbb{M}}\{\lambda_i\}$, $\xi=\max_{i\in\mathbb{M}}\{\xi_i\}$, $\bar{\lambda}=\max_{i\in\mathbb{M}}\{\bar{\lambda}_i\}$, $\lambda_i=2\left(d_i-\Lambda-\sum_{j=1}^{m}a_{ij}\delta_{ij}\right)>0$, $\bar{\lambda}_i=2\left(\Lambda+\sum_{j=1}^{m}a_{ij}\delta_{ij}\right)$, $\xi_i=2\sum_{j=1}^{m}a_{ij}\delta_{ij}$, $\Lambda=\max\left\{\check{Q}_1,\check{Q}_2,\check{Q}_3\right\}$, $\check{Q}_1=-\alpha_1+\frac{(\alpha_1+\alpha_2+p_3)Q}{2}+\frac{\eta p_2}{2}$, $\check{Q}_2=\alpha_3+\frac{\alpha_1+\alpha_2+p_3}{2Q}$, $\check{Q}_3=\frac{p_2}{2\eta}-\alpha_4$, *and Q, η are arbitrary positive constants.*

Proof. By simple calculation, we can derive that

$$\begin{aligned}
&(x_i-s)^{\mathrm{T}}[f(x_i,\tilde{x}_i)-f(s,\tilde{s})]\\
&=(e_{i1},e_{i2},e_{i3})\begin{pmatrix}\alpha_1(e_{i1}-e_{i2})\\ \alpha_2e_{i1}+\alpha_3e_{i2}-s_1e_{i3}-e_{i1}e_{i3}\\ e_{i1}e_{i2}-\alpha_4e_{i3}-s_1e_{i2}+s_2e_{i1}\end{pmatrix}\\
&=-\alpha_1e_{i1}^2+\alpha_3e_{i3}^2+(\alpha_1+\alpha_2-s_3)e_{i1}e_{i2}+s_2e_{i1}e_{i3}\\
&\le-\alpha_1e_{i1}^2+\alpha_3e_{i2}^2-\alpha_4e_{i3}^2+(\alpha_1+\alpha_2+p_3)|e_{i1}e_{i2}|+p_2|e_{i1}e_{i3}|\\
&\le\left(-\alpha_1+\frac{(\alpha_1+\alpha_2+p_3)Q}{2}+\frac{\eta p_2}{2}\right)e_{i1}^2+\left(\alpha_3+\frac{\alpha_1+\alpha_2+p_3}{2Q}\right)e_{i2}^2\\
&\quad+\left(\frac{p_2}{2\eta}-\alpha_4\right)e_{i3}^2\\
&\le\max\left\{\check{Q}_1,\check{Q}_2,\check{Q}_3\right\}|e_i|^2,
\end{aligned}$$

which means condition B1 in Theorem 2 is satisfied. Combined with conditions in Theorem 3, it is evident that all conditions in Theorem 2 are satisfied. Hence, according to Theorem 2, system (16) can achieve global synchronization. This completes the proof. □

4.2. Synchronization of fractional-order coupled Hindmarsh–Rose neuron systems with time-varying delays

In this subsection, we will apply our theoretical results to FOCHRNSs with time-varying delays. The Hindmarsh–Rose model was first proposed by Hindmarsh and Rose, which can qualitatively represent the firing behaviors of neurons. According to [41], the Hindmarsh–Rose neuron systems in fractional-order can be depicted as

$$\begin{cases}\mathrm{D}^\alpha x_{i1}(t)=x_{i2}(t)-ax_{i1}^3(t)+bx_{i1}^2(t)-x_{i3}(t)+I_{ext},\\ \mathrm{D}^\alpha x_{i2}(t)=c-dx_{i1}^2(t)-x_{i2}(t), & i\in\mathbb{M},\\ \mathrm{D}^\alpha x_{i3}(t)=r(S(x_{i1}(t)-\bar{x})-x_{i3}(t)),\end{cases}$$

where $x_{i1}(t)$ stands for the membrane action potential, $x_{i2}(t)$ is the recovery variable, $x_{i3}(t)$ represents the associated slow adaptation current, $0<\alpha<1$ is the order of fractional-order, and I_{ext} is the external current intensity. Here, $a,b,c,d,S,r,\bar{x}$, and I_{ext} are real constants.

Let $x_i(t)=(x_{i1}(t),x_{i2}(t),x_{i3}(t))^{\mathrm{T}}$ be the ith state vector. Likewise, taking nonlinear coupling, time-varying coupling delay and periodically intermittent controller into consideration, FOCHRNSs with time-varying delays are given as

$$\begin{aligned}\mathrm{D}^\alpha x_i(t)&=\tilde{f}(x_i(t),x_i(t-\tau_1(t)))+\sum_{j=1}^m a_{ij}H_{ij}(x_j(t-\tau_2(t))\\ &\quad-x_i(t-\tau_2(t)))+u_i(t),\quad i\in\mathbb{M},\end{aligned}\tag{17}$$

where $\tilde{f}(x_i(t),x_i(t-\tau_1(t)))=(x_{i2}(t)-ax_{i1}^3(t)+bx_{i1}^2(t)-x_{i3}(t)+I_{ext},c-dx_{i1}^2(t)-x_{i2}(t),r(S(x_{i1}(t)-\bar{x})-x_{i3}(t)))^{\mathrm{T}}$, the nonnegative constant a_{ij} stands for the coupling strength, $H_{ij}:\mathbb{R}^3\to\mathbb{R}^3$ is the coupling form, $\tau_1(t)=0$, $\tau_2(t)$ is the time-varying coupling delay which is bounded by a positive constant τ, that is $0\le\tau_2(t)\le\tau$.

Let $s(t)=(s_1(t),s_2(t),s_3(t))^{\mathrm{T}}$, and suppose that $s(t)$ is a solution of an isolated node which satisfies

$$\mathrm{D}^\alpha s(t)=\tilde{f}(s(t),s(t-\tau_1(t))).$$

Since a chaotic system has bound trajectories, there is a positive constant P, such that $|x_{ij}|,|s_i|\le P, i\in\mathbb{M}, j=1,2,3$. Moreover, define the synchronization error $e_i(t)=x_i(t)-s(t), i\in\mathbb{M}$. Notice that

$$\begin{aligned}
&(x_i-s)^{\mathrm{T}}[\tilde{f}(x_i,\tilde{x}_i)-\tilde{f}(s,\tilde{s})]\\
&=(e_{i1},e_{i2},e_{i3})\begin{pmatrix}e_{i2}-e_{i3}-ae_{i1}(x_{i1}^2+x_{i1}s_1+s_1^2)+be_{i1}(x_{i1}+s_1)\\ -e_{i2}-de_{i1}(x_{i1}+s_1)\\ rSe_{i1}-re_{i3}\end{pmatrix}\\
&\le(2Pb+3P^2a)e_{i1}^2-e_{i2}^2-re_{i3}^2+(rS+1)|e_{i1}e_{i3}|+(1+2Pd)|e_{i1}e_{i2}|\\
&\le\left(2Pb+3P^2a+\frac{1}{2}rS+Pd+1\right)e_{i1}^2+\left(Pd-\frac{1}{2}\right)e_{i2}^2+\left(\frac{1}{2}(rS+1)-r\right)e_{i3}^2\\
&\le\max\left\{\check{S}_1,\check{S}_2,\check{S}_3\right\}|e_i|^2,
\end{aligned}$$

where $\check{S}_1=2Pb+3P^2a+\frac{1}{2}rS+Pd+1$, $\check{S}_2=Pd-\frac{1}{2}$, $\check{S}_3=\frac{1}{2}(rS+1)-r$ are positive constants. Hence, it is easy to obtain that condition B1 in Theorem 2 is satisfied.

Subsequently, the error system can be expressed as follows

$$\begin{aligned}\mathrm{D}^\alpha e_i(t)&=\tilde{f}(x_i(t),x_i(t-\tau_1(t)))-\tilde{f}(s(t),s(t-\tau_1(t)))\\ &\quad+\sum_{j=1}^m a_{ij}H_{ij}(x_j(t-\tau_2(t))-x_i(t-\tau_2(t)))+u_i(t),\quad i\in\mathbb{M}.\end{aligned}$$

In what follows, we present a theorem to ensure the synchronization of system (17).

Theorem 4. *Suppose that Assumption 1 is satisfied, and digraph $(\mathcal{G},A)$, where $A=(a_{ij})_{m\times m}$, is strongly connected. System (17) can reach global synchronization if there exist positive constants θ_1 and θ_2 such that*

$$E_\alpha[-\theta_1\varpi^\alpha T^\alpha]E_\alpha[\theta_2(1-\varpi)^\alpha T^\alpha]<1,$$

where $\lambda-2\xi\ge\theta_1$, $\bar{\lambda}+2\xi\le\theta_2$, $\lambda=\min_{i\in\mathbb{M}}\{\lambda_i\}$, $\xi=\max_{i\in\mathbb{M}}\{\xi_i\}$, $\bar{\lambda}=\max_{i\in\mathbb{M}}\{\bar{\lambda}_i\}$, $\lambda_i=2\left(d_i-\Lambda-\sum_{j=1}^m a_{ij}\delta_{ij}\right)>0$, $\bar{\lambda}_i=2\left(\Lambda+\sum_{j=1}^m a_{ij}\delta_{ij}\right)$, $\xi_i=2\sum_{j=1}^m a_{ij}\delta_{ij}$, $\Lambda=\max\left\{\check{S}_1,\check{S}_2,\check{S}_3\right\}$, $\check{S}_1=2Pb+3P^2a+\frac{1}{2}rS+Pd+1$, $\check{S}_2=Pd-\frac{1}{2}$, $\check{S}_3=\frac{1}{2}(rS+1)-r$.

To conserve space, we here omit the proof of Theorem 4. They can be directly derived by Theorem 2 since all the conditions can be verified easily.

5. Numerical simulations

In this section, for the purpose of illustrating the effectiveness of theoretical results and showing the feasibility of periodically intermittent control, numerical simulations are given as follows.

Example 1. As a specific example of unified fractional-order chaotic systems, fractional-order Lorenz systems are considered.

Taking nonlinear coupling, time-varying delays and periodically intermittent controller into account, fractional-order Lorenz coupled systems with time-varying delays, which are modeled on digraph $(\mathcal{G},A)$ with 10 nodes (see Fig. 1), can be described by

$$\begin{aligned}\mathrm{D}^\alpha x_i(t)&=f(x_i(t),x_i(t-\tau_1(t)))+\sum_{j=1}^{10}a_{ij}H_{ij}(x_j(t-\tau_2(t))\\ &\quad-x_i(t-\tau_2(t)))+u_i(t),\quad i\in\{1,2,\ldots,10\},\end{aligned}\tag{18}$$

where $f(x_i(t),x_i(t-\tau_1(t)))=\begin{pmatrix}10(x_{i2}(t)-x_{i1}(t))\\ 28x_{i1}(t)-x_{i1}(t)x_{i3}(t)+x_{i2}(t)\\ x_{i1}(t)x_{i2}(t)-\frac{8}{3}x_{i3}(t)\end{pmatrix}$, $\alpha=0.994$, $H_{ij}(x)=\sin x$, $\tau_1(t)=0$, $\tau_2(t)=0.01\sin^2 t$ and the nonzero elements of weight matrix $A=(a_{ij})_{10\times10}$ is given as

$a_{17}=0.01, a_{28}=0.02, a_{39}=0.03, a_{4,10}=0.04, a_{56}=0.015,$
$a_{61}=0.014, a_{67}=0.017, a_{72}=0.016,$

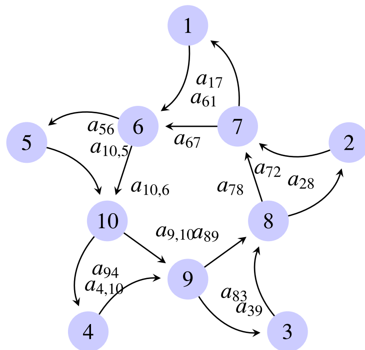

Fig. 1. Digraph $(\mathcal{G}, A)$ with 10 nodes.

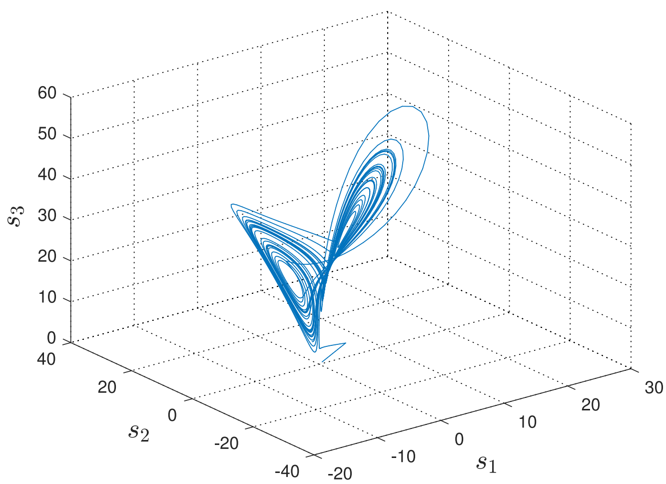

Fig. 2. The attractor of system (19).

$a_{78} = 0.019$, $a_{83} = 0.018$, $a_{89} = 0.021$, $a_{94} = 0.02$, $a_{10,5} = 0.022$, $a_{10,6} = 0.024$, $a_{9,10} = 0.023$.

Obviously, digraph $(\mathcal{G}, A)$ is strongly connected. Suppose that $s(t)$ is a solution of an isolated node which satisfies

$$D^{\alpha}s(t) = f(s(t), s(t - \tau_1(t))). \tag{19}$$

The attractor of system (19) is depicted in Fig. 2, and we can find that $|s_1(t)| \leq 21$, $|s_2(t)| \leq 28$ and $|s_3(t)| \leq 52$.

Choose $Q = 1.1$, $\eta = 1$, by simple calculation, we can derive that $\check{Q}_1 = 39.5$, $\check{Q}_2 = 41.9091$ and $\check{Q}_3 = 11.3333$. It follows that $\Lambda = 41.9091$. The periodically intermittent controller $u_i(t)$ in system (18) is given as

$$u_i(t) = \begin{cases} -80(x_i(t) - s(t)), & lT \leq t \leq (l+\varpi)T, \\ 0, & (l+\varpi)T < t < (l+1)T, \end{cases} \quad l \in \mathbb{N}, i \in \{1, 2, \ldots, 10\},$$

and set $T = 0.1$ and $\varpi = 0.6$. Through a direct computation, the values of parameters λ_i, $\bar{\lambda}_i$ and ξ_i are listed in Table 1.

Hence, we have $\lambda = 76.0898$, $\bar{\lambda} = 83.7982$ and $\xi = 0.0920$. Let $\theta_1 = \lambda - 2\xi = 75.9058$, $\theta_2 = \bar{\lambda} + 2\xi = 83.9822$. Though computing,

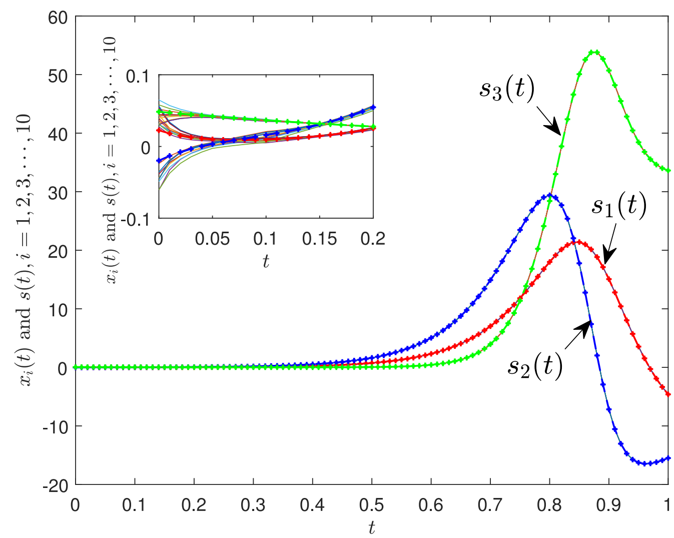

Fig. 3. The state trajectories of systems (18) and (19).

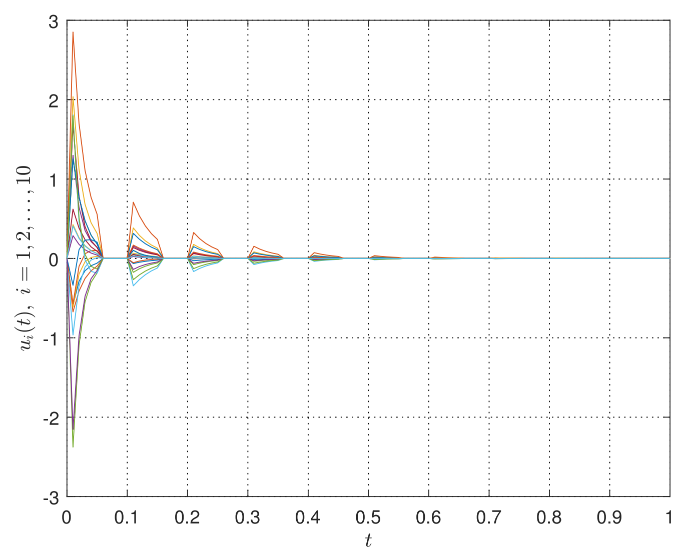

Fig. 4. Time evolution of periodically intermittent control (5).

it is clear that

$$E_{\alpha}[-\theta_1 \varpi^{\alpha} T^{\alpha}] E_{\alpha}[\theta_2 (1 - \varpi)^{\alpha} T^{\alpha}] = 0.3702 < 1.$$

Up to now, all conditions in Theorem 3 are satisfied.

Fig. 3 depicts the state trajectories of systems (18) and (19). Fig. 4 displays the time evolution of periodically intermittent control (5). Moreover, Fig. 5 depicts the state trajectories of synchronization errors between systems (18) and (19), which shows that the errors tend to zero as time increases. And synchronization errors in logarithmic coordinates are presented in Fig. 6. Namely, system (18) can reach global synchronization. Hence, it is consistent with the result of Theorem 3, and our theoretical results are further validated.

Table 1
The values of parameters λ_i, $\bar{\lambda}_i$ and ξ_i.

	$i=1$	$i=2$	$i=3$	$i=4$	$i=5$	$i=6$	$i=7$	$i=8$	$i=9$	$i=10$
λ_i	76.1618	76.1418	76.1218	76.1018	76.1518	76.1198	76.1118	76.1038	76.0958	76.0898
$\bar{\lambda}_i$	83.7982	83.7782	83.7582	83.7382	83.7882	83.7562	83.7482	83.7402	83.7322	83.7262
ξ_i	0.0200	0.0400	0.0600	0.0800	0.0300	0.0620	0.0700	0.0780	0.0860	0.0920

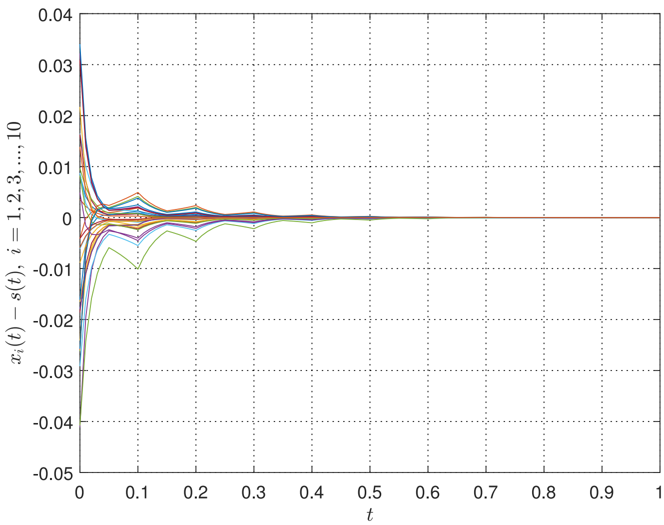

Fig. 5. The state trajectories of synchronization errors between systems (18) and (19).

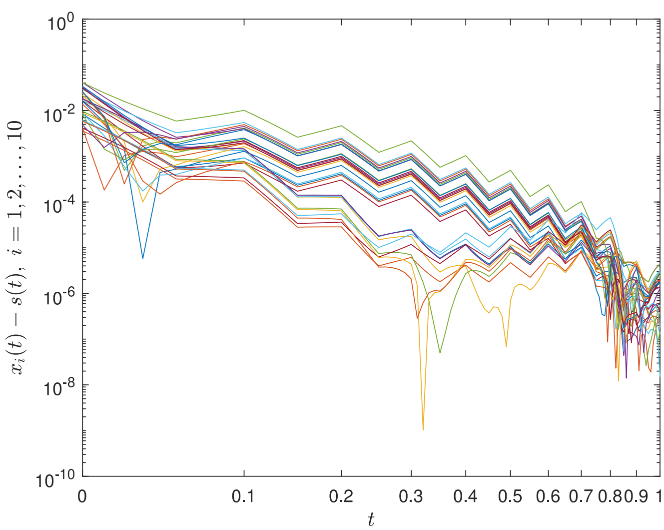

Fig. 6. Synchronization errors in logarithmic coordinates between systems (18) and (19).

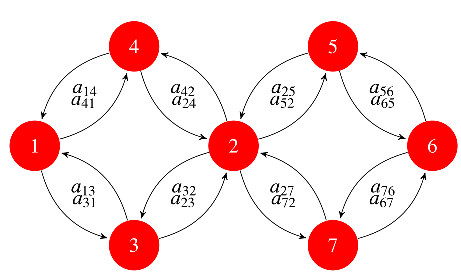

Fig. 7. Digraph $(\mathcal{G}, A)$ with 7 nodes.

Example 2. Consider FOCHRNSs with time-varying delays modeled on a digraph with 7 nodes (see Fig. 7), which can be expressed by

$$\begin{aligned} \mathrm{D}^\alpha x_i(t) = {} & \tilde{f}(x_i(t), x_i(t-\tau_1(t))) + \sum_{j=1}^{7} a_{ij} H_{ij}(x_j(t-\tau_2(t)) \\ & - x_i(t-\tau_2(t))) + u_i(t), \quad i \in \{1, 2, \ldots, 7\}, \end{aligned} \tag{20}$$

where $\alpha = 0.9$, $a = 1$, $b = 3$, $c = 1$, $d = 5$, $S = 4$, $r = 0.006$, $\bar{x} = 1.56$, $I_{ext} = 2$, $H_{ij}(x) = \cos x$, $\tau_1(t) = 0$, $\tau_2(t) = 0.01$. The nonzero elements of the weight matrix $A = (a_{ij})_{7\times 7}$ are provided as below

$a_{13} = 0.012$, $a_{14} = 0.064$, $a_{23} = 0.071$, $a_{24} = 0.052$, $a_{25} = 0.041$,
$a_{27} = 0.086$, $a_{31} = 0.097$, $a_{32} = 0.019$,
$a_{41} = 0.021$, $a_{42} = 0.046$, $a_{52} = 0.017$, $a_{56} = 0.025$, $a_{65} = 0.014$,
$a_{67} = 0.068$, $a_{72} = 0.079$, $a_{76} = 0.091$.

Clearly, digraph $(\mathcal{G}, A)$ is strongly connected. Furthermore, the solution of an isolated node satisfies

$$\mathrm{D}^\alpha s(t) = \tilde{f}(s(t), s(t-\tau_1(t))), \tag{21}$$

which is shown in Fig. 8. Additionally, the periodically intermittent controller $u_i(t)$ is designed as

$$u_i(t) = \begin{cases} -75(x_i(t) - s(t)), & lT \le t \le (l+\varpi)T, \\ 0, & (l+\varpi)T < t < (l+1)T, \end{cases} \quad l \in \mathbb{N}, i \in \{1, 2, \ldots, 7\},$$

and set $T = 0.1$ and $\varpi = 0.8$. Through simulations, we can derive that $P = 2.5$, $\check{S}_1 = 47.262$, $\check{S}_2 = 12$, $\check{S}_3 = 0.506$, which indicates that $\Lambda = 47.262$. By calculations, the values of parameters λ_i, $\bar{\lambda}_i$ and ξ_i are presented in Table 2. Hence, we can obtain $\lambda = 54.976$, $\bar{\lambda} = 95.024$ and $\xi = 0.5$. Let $\theta_1 = \lambda - 2\xi = 53.976$, $\theta_2 = \bar{\lambda} + 2\xi = 96.024$. By computing, it is clear that

$$E_\alpha[-\theta_1 \varpi^\alpha T^\alpha] E_\alpha[\theta_2 (1-\varpi)^\alpha T^\alpha] = 0.7819 < 1.$$

Up to now, all conditions in Theorem 4 are satisfied.

The state trajectories of synchronization errors between systems (20) and (21) are shown in Fig. 9, from which, we can notice that the errors tend to zero with time evolution. And the synchronization errors in logarithmic coordinates between systems (20) and (21) are displayed in Fig. 10. That is to say, system (20) can achieve synchronization under periodically intermittent control. Likewise, numerical simulations are in agreement with the results of Theorem 4, which validates our theoretical results.

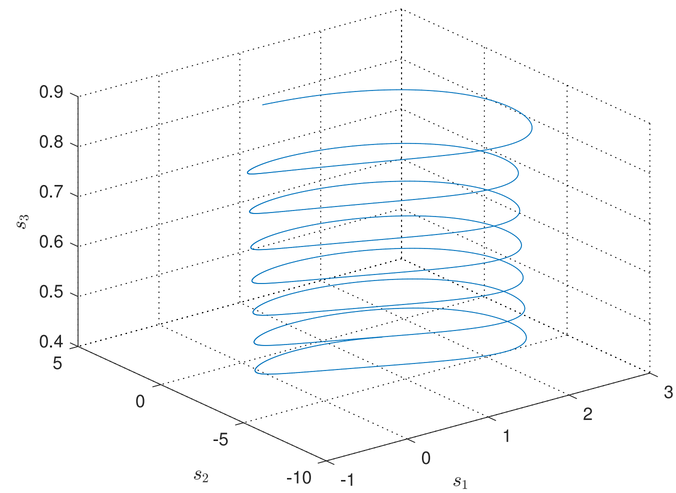

Fig. 8. The phase diagram of system (21).

Table 2
The values of parameters λ_i, $\bar{\lambda}_i$ and ξ_i.

	$i=1$	$i=2$	$i=3$	$i=4$	$i=5$	$i=6$	$i=7$
λ_i	55.3240	54.9760	55.2440	55.3420	55.3920	55.3120	55.1360
$\bar{\lambda}_i$	94.6760	95.0240	94.7560	94.6580	94.6080	94.6880	94.8640
ξ_i	0.1520	0.5000	0.2320	0.1340	0.0840	0.1640	0.3400

6. Conclusion

In this paper, synchronization problem of FOCSs with time-varying delays via periodically intermittent control was investigated. On the one hand, nonlinear coupling, time-varying internal delay and time-varying coupling delay were considered in our

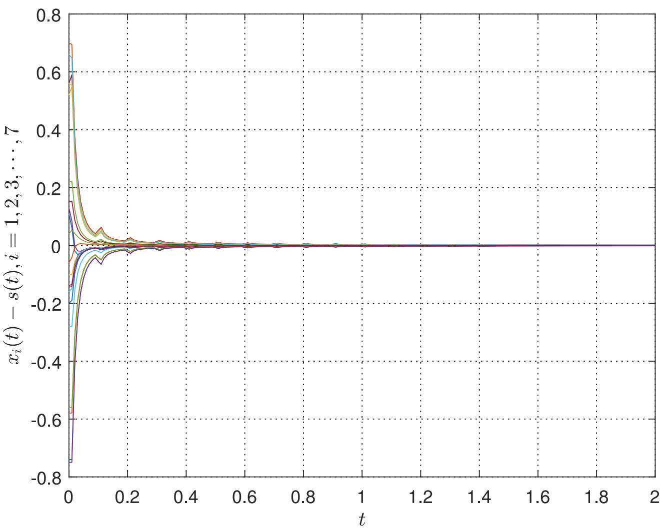

Fig. 9. The state trajectories of synchronization errors between systems (20) and (21).

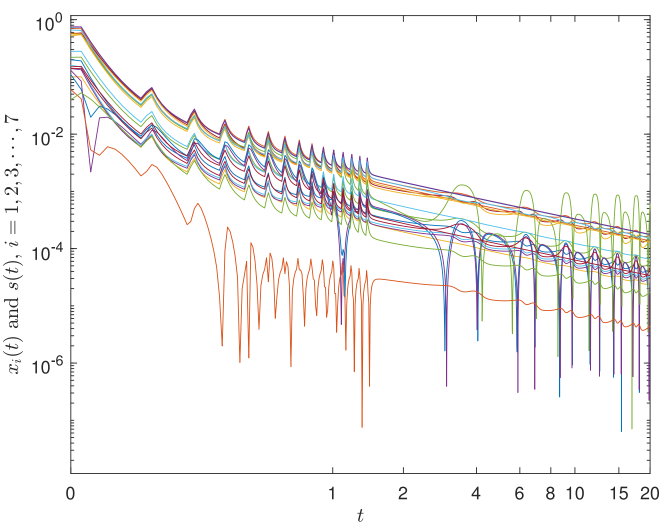

Fig. 10. Synchronization errors in logarithmic coordinates between systems (20) and (21).

models. On the other hand, periodically intermittent control strategy was adopted to synchronize FOCSs with time-varying delays for the first time. Moreover, by combining Lyapunov method with graph-theoretic approach, some synchronization criteria for FOCSs with time-varying delays were derived. In particular, synchronization of FOCCSs and FOCHRNSs with time-varying delays were investigated as applications. Numerical simulations with regard to fractional-order Lorenz coupled systems and FOCHRNSs with time-varying delays were presented to verify the effectiveness of our theoretical results. It is worthwhile noting that the strong connectedness of digraph is a prerequisite in our theoretical results. Thereby, we will make an attempt to investigate synchronization of FOCSs when digraph is not strongly connected in the future. Furthermore, aperiodically intermittent control strategy will also be considered in our future work.

Acknowledgments

The authors really appreciate the valuable comments of the editors and reviewers. This work was supported by Shandong Province Natural Science Foundation (nos. ZR2018MA005, ZR2018MA020, ZR2017MA008); the Key Project of Science and Technology of Weihai (no. 2014DXGJMS08) and the Innovation Technology Funding Project in Harbin Institute of Technology (no. HIT.NSRIF.201703).

Appendix A

Some basic concepts and a lemma on graph theory will be introduced in the following, which can be found in [7,42].

A digraph $\mathcal{G} = (\mathbb{M}, \mathbb{E})$ contains a set $\mathbb{M}$ of nodes and a set $\mathbb{E}$ of arcs (j, i) which leads from initial node j to terminal node i. If each arc (j, i) is assigned a positive weight a_{ij}, then digraph $\mathcal{G}$ is weighted. There exists an arc (j, i) in $\mathcal{G}$ if and only if $a_{ij} > 0$. The weight $W(\mathcal{H})$ of a subgraph $\mathcal{H}$ is equal to the product of the weights on all its arcs. A directed path $\mathcal{P}$ in $\mathcal{G}$ is a subgraph with distinct nodes $i_1, i_2, \ldots, i_m$ such that its set of arcs is $(i_k, i_{k+1}) : k = 1, 2, \ldots, m-1$. If $i_m = i_1$, $\mathcal{P}$ is called to a directed cycle. If for any pair of distinct nodes of digraph $\mathcal{G}$, there exists a directed path from one to the other, then digraph $\mathcal{G}$ is strongly connected. For a weighted digraph $\mathcal{G}$ with n nodes, define the weight matrix $A = (a_{ij})_{m\times m}$ whose entry a_{ij} equals the weight of arc (j, i), and $a_{ij} = 0$ if there exists no arc (j, i). The digraph $\mathcal{G}$ with weight matrix A is denoted as $(\mathcal{G}, A)$. Define the Laplacian matrix of $(\mathcal{G}, A)$ as $\mathbb{L} = (p_{ij})_{m\times m}$, where $p_{ij} = \sum_{k\neq i} a_{ik}$ for $i = j$ and $p_{ij} = -a_{ij}$ for $i \neq j$. Denote directed cycle of unicyclic graph $\mathcal{Q}$ as $\mathcal{C}_{\mathcal{Q}}$.

Lemma 2. *Suppose that $m \geq 2$ and $(\mathcal{G}, A)$, in which $A = (a_{ij})_{m\times m}$, is a weighted digraph. Let c_i be the cofactor of the ith diagonal element of $\mathbb{L}$,and the set of all spanning unicyclic graphs $\mathcal{Q}$ of $(\mathcal{G}, A)$ are denoted as $\mathbb{Q}$. Then for arbitrary functions $F_{ij}(e_i, e_j)$, $i, j \in \mathbb{M}$, the following equation holds.*

$$\sum_{i,j=1}^{m} c_i a_{ij} F_{ij}(e_i, e_j) = \sum_{\mathcal{Q}\in\mathbb{Q}} W(\mathcal{Q}) \sum_{(s,r)\in\mathbb{E}(\mathcal{C}_{\mathcal{Q}})} F_{rs}(e_r, e_s),$$

where $W(\mathcal{Q})$ is the weight of $\mathcal{Q}$, and $\mathcal{C}_{\mathcal{Q}}$ stands for the directed cycle of $\mathcal{Q}$. In addition, if digraph $(\mathcal{G}, A)$ is strongly connected, then $c_i > 0$.

References

[1] Rakkiyappan R, Latha VP, Zhu QX, Yao ZS. Exponential synchronization of Markovian jumping chaotic neural networks with sampled-data and saturating actuators. Nonlinear Anal-Hybrid Syst 2017;24:28–44.

[2] Tang Y, Gao HJ, Lu JQ, Kurths J. Pinning distributed synchronization of stochastic dynamical networks: a mixed optimization approach. IEEE Trans Neural Netw Learn Syst 2014;25(10):1804–15.

[3] Wang JL, Qin Z, Wu HN, Huang TW. Finite-time synchronization and $\mathcal{H}_\infty$ synchronization of multi-weighted complex networks with adaptive state couplings. IEEE T Cybern 2018. doi:10.1109/tcyb.2018.2870133.

[4] Shi L, Yang HL, Wang X, Zhong SM, Wang WQ. Synchronization of complex networks with asymmetric coupling via decomposing matrix method. Chaos Solitons Fractals 2018;111:180–5.

[5] Yang WG, Yu WW, Cao JD. Global exponential stability of impulsive fuzzy high--order BAM neural networks with continuously distributed delays. IEEE Trans Neural Netw Learn Syst 2017;29(8):3682–700.

[6] Fan YH, Liu HM, Zhu YG, Mei J. Fast synchronization of complex dynamical networks with time-varying delay via periodically intermittent control. Neurocomputing 2016;205:182–94.

[7] Li MY, Shuai ZS. Global-stability problem for coupled systems of differential equations on networks. J Differ Equ 2010;248(1):1–20.

[8] Wu YB, Li Q, Li WX. Novel aperiodically intermittent stability criteria for Markovian switching stochastic delayed coupled systems. Chaos 2018;28:113117.

[9] Wang PF, Hong Y, Su H. Stabilization of stochastic complex-valued coupled delayed systems with Markovian switching via periodically intermittent control. Nonlinear Anal-Hybrid Syst 2018;29:395–413.

[10] Liu Y, Li WX, Feng JQ. The stability of stochastic coupled systems with time–varying coupling and general topology structure. IEEE Trans Neural Netw Learn Syst 2018;29(9):4189–200.

[11] Ding YS, Wang ZD, Ye HP. Optimal control of a fractional-order HIV-immune system with memory. IEEE Trans Control Syst Technol 2012;20(3):763–9.

[12] Bao HB, Park JH, Cao JD. Adaptive synchronization of fractional-order memristor-based neural networks with time delay. Nonlinear Dyn 2015;82(3):1343–54.

[13] Stamova I. Global Mittag-Leffler stability and synchronization of impulsive fractional-order neural networks with time-varying delays. Nonlinear Dyn 2014;77(4):1251–60.

[14] Behinfaraz R, Badamchizadeh MA, Ghiasi AR. An approach to achieve modified projective synchronization between different types of fractional-order chaotic systems with time-varying delays. Chaos Solitons Fractals 2015;78:95–106.

[15] Li HL, Cao JD, Jiang HJ, Alsaedi A. Graph theory-based finite-time synchronization of fractionalorder complex dynamical networks. J Frankl Inst-Eng Appl Math 2018;355(13):5771–89.

[16] Mehrdad S, Mahdi P. Robust fixed-time synchronization of fractional order chaotic using free chattering nonsingular adaptive fractional sliding mode controller design. Chaos Solitons Fractals 2018;113:135–47.

[17] Chen JJ, Zeng ZG, Jiang P. Global mittag-leffler stability and synchronization of memristor-based fractional-order neural networks. Neural Netw 2014;51:1–8.

[18] Liu M, Fan M. Stability in distribution of a three-species stochastic cascade predator-prey system with time delays. IMA J Appl Math 2017;82:396–423.

[19] Liang S, Wu RC, Chen LP. Adaptive pinning synchronization in fractional-order uncertain complex dynamical networks with delay. Physica A 2016;444:49–62.

[20] Wu X, Liu S, Yang R, Zhang YJ, Li XY. Global synchronization of fractional complex networks with non-delayed and delayed couplings. Neurocomputing 2018;290:43–9.

[21] Ma TD, Zhang J, Zhou YC, Wang HY. Adaptive hybrid projective synchronization of two coupled fractional-order complex networks with different sizes. Neurocomputing 2015;164:182–9.

[22] Liu YJ, Guo BZ, Park JH, Lee SM. Nonfragile exponential synchronization of delayed complex dynamical networks with memory sampled-data control. IEEE Trans Neural Netw Learn Syst 2018;29(1):118–28.

[23] He WL, Qian F, Cao JD. Pinning-controlled synchronization of delayed neural networks with distributed-delay coupling via impulsive control. Neural Netw 2017;85:1–9.

[24] Feng JW, Yang P, Zhao Y. Cluster synchronization for nonlinearly time-varying delayed coupling complex networks with stochastic perturbation via periodically intermittent pinning control. Appl Math Comput 2017;291:52–68.

[25] Xu Y, Zhou H, Li WX. Stabilisation of stochastic delayed systems with Lévy noise on networks via periodically intermittent control. Int J Control 2018. doi:10.1080/00207179.2018.1479538.

[26] Liu Y, Sun LJ, Lu JQ, Liang JL. Feedback controller design for the synchronization of boolean control networks. IEEE Trans Neural Netw Learn Syst 2017;27(9):1991–6.

[27] Li HL, Hu C, Jiang HJ, Teng ZD, Jiang YL. Synchronization of fractional-order complex dynamical networks via periodically intermittent pinning control. Chaos Solitons Fractals 2017;103:357–63.

[28] Zhang LZ, Yang YQ, Wang F. Lag synchronization for fractional-order memristive neural networks via period intermittent control. Nonlinear Dyn 2017;89(1):367–81.

[29] Wan P, Jian JG, Mei J. Periodically intermittent control strategies for α-exponential stabilization of fractional-order complex-valued delayed neural networks. Nonlinear Dyn 2018;92(2):247–65.

[30] Peng X, Wu HQ, Song K, Shi JX. Global synchronization in finite time for fractional-order neural networks with discontinuous activations and time delays. Neural Netw 2017;94:46–54.

[31] Stamov IM, Simeonov S. Delayed reaction-diffusion cellular neural networks of fractional order: Mittag-Leffler stability and synchronization. J Comput Nonlinear Dyn 2018;13(1):011015.

[32] Stamova I, Stamova G. Mittag-leffler synchronization of fractional neural networks with time-varying delays and reaction-diffusion terms using impulsive and linear controllers. Neural Netw 2017;96:22–32.

[33] Wang F, Yang YQ, Hu AH, Xu XY. Exponential synchronization of fractional-order complex networks via pinning impulsive control. Nonlinear Dyn 2015;82(4):1979–87.

[34] Yang XJ, Li CD, Huang TW, Song QK, Huang JJ. Global Mittag-Leffler synchronization of fractional-order neural networks via impulsive control. Neural Process Lett 2018;48(1):459–79.

[35] Zheng MW, Li LX, Peng HP, Xiao JH, Yang YX, Zhang YP, Zhao H. Finite-time stability and synchronization of memristor-based fractional-order fuzzy cellular neural networks. Commun Nonlinear Sci Numer Simul 2018;59:272–91.

[36] Yang XJ, Li CD, Huang TW, Chen XF. Quasi-uniform synchronization of fractional-order memristor-based neural networks with delay. Neurocomputing 2017;234:205–15.

[37] Chen LP, Cao JD, Wu RC, Machado JAT, Lopes AM, Yang HJ. Stability and synchronization of fractional-order memristive neural networks with multiple delays. Neural Netw 2017;94:76–85.

[38] Zhang S, Yu YG, Yu JZ. LMI conditions for global stability of fractional-order neural networks. IEEE Trans Neural Netw Learn Syst 2017;28(10):2423–33.

[39] Yang Y, He Y, Wang Y, Mu M. Stability analysis of fractional-order neural networks: an LMI approach. Neurocomputing 2018;285:82–93.

[40] Li CG, Liao XF, Yu JB. Synchronization of fractional order chaotic systems. Phys Rev E 2003;68(6-2):067203.

[41] Dong J, Zhang GJ, Xie Y, Yao H, Wang J. Dynamic behavior analysis of fractional-order Hindmarsh–Rose neuronal model. Cogn Neurodyn 2014;8:167–75.

[42] West DB. Introduction to graph theory. Upper Saddle River: Prentice Hall; 1996.